Preparation and degradation properties of $AgBiS_2$/BiOI composite photocatalytic materials with high catalytic activity

Y. L. Zhuang[a], X. H. Zhang[a], L. M. Dong[a,*], Y. Li[b], D. Li[a], J. H. Dong[a], Z. W. Liu[a], S. Tian[a], L. M. Wang[a], Y. Dai[c,]

[a]*Heilongjiang Provincial Key Laboratory of CO_2 Resource Utilization and Energy Catalytic Materials, School of Material Science and Chemical Engineering, Harbin University of Science and Technology, Harbin, 150040, China*

[b]*Guangxi Key Laboratory of Optical and Electronic Materials and Devices, Guilin University of Technology, Guilin, China*

[c]*Department of Industry Engineering，Harbin Institute of Technology，Harbin 150001，China*

An $AgBiS_2$/BiOI composites with different proportions were prepared by precipitation method, and their catalytic activity was studied by degrading RhB (100 mg/L) under simulated light conditions. The results showed that the photocatalytic activity of $AgBiS_2$/BiOI composite was the best when the doping amount of $AgBiS_2$ was 4 wt. % (the degradation rate was about 94%). Compared with pure BiOI, the degradation rate of RhB increased by 24%. After 5 cycles of experiments, the degradation rate of the material can still reach 94%, indicating that the $AgBiS_2$/BiOI composite has good stability.

(Received January 13, 2022; Accepted June 23, 2022)

Keywords: Photocatalyst, $AgBiS_2$/BiOI, Catalytic mechanism, Rhodamine B

1. Introduction

In contemporary society, the increasing industrialisation and urbanisation has led to a serious shortage of clean water resources as dye wastewater discharged from various industries (e.g. paper industry, textile dyeing, cosmetics, etc.) enters the natural water cycle [1]. For the environment, the treatment and recycling of dye wastewater can increase the limited supply of fresh water in the long run [2]. Although conventional wastewater treatment technologies can eliminate pollutants from dye wastewater in the short term, they can cause secondary pollution as well as the production of some life-threatening bacteria or soluble organic compounds [3,4]. In contrast, the emerging semiconductor photocatalytic oxidation reduction has good prospects for application as a green and sustainable method for removing pollutants from dye wastewater [5-7].

Bismuth photocatalysts have attracted great interest from researchers due to their abundant species, unique electronic structure, excellent visible light absorption ability and high degradation ability of organic matter. Bismuth iodide oxide has attracted extensive attention due to its unique layered structure and good visible light photocatalytic activity [8].This is because BiOX with layered structure has enough space to polarize corresponding atoms and atomic orbitals. This induced dipole moment can effectively separate holes and electrons, which is conducive to improving the photocatalytic performance of the material [9]. Moreover, BiOX (X=Cl, Br, I) is an indirect transition band gap, so the excited electrons must pass through some K layers to reach the valence band, which reduces the probability of recombination of excited electrons and holes. The simultaneous existence of open structure and indirect transition mode is conducive to the effective separation and charge transfer of hole-electron pairs. These characteristics are the basis for the high photocatalytic activity of BiOX(X=Cl, Br, I) [10]. The band gap of BiOX system decreased gradually with F, Cl, Br and I. Among them, the band gap with BiOCl is about 3.2 eV, that with BiOBr is about 2.7 eV, and that with BiOI is about 1.7 eV. In contrast, BiOI has the narrowest

* Corresponding author: donglm@hrbust.edu.cn
https://doi.org/10.15251/DJNB.2022.172.685

band gap, which is conducive to the generation of photogenic electron hole pairs in the material [11]. However, the photocatalytic performance of BiOI was affected by the rapid recombination rate of electron-hole pairs generated in the photocatalytic application process [12]. In order to improve the photocatalytic performance of BiOI materials, many composites of BiOI have been investigated, such as BiOI/g-C_3N_4 [13], BiOI/MoS_2 [14], Bi_2WO_6/BiOI [15], Co_3O_4/BiOI [16], etc.

In recent years, ternary sulfides (TCs) with Ⅰ-Ⅲ-Ⅵ structure have received extensive attention in the field of optoelectronics due to their excellent optoelectronic properties, higher light absorption capacity and excellent light absorption rate [17,18]. Among them, $AgBiS_2$ is a common bismuth sulphide compound in TCs, which often exists as hexagonal phase ß-$AgBiS_2$ (low temperature phase) and cubic phase α-$AgBiS_2$ (high temperature phase), of which both have a phase transition temperature of 195°C [19]. The material has received increasing attention in energy conversion due to its own optoelectronic properties such as high absorption coefficient (104-105 cm^{-1}) and tunable forbidden band width [20]. Researchers have compounded $AgBiS_2$ with other materials to prepare heterojunctions, such as $AgBiS_2/TiO_2$ [21] and $AgBiS_2/Bi_2O_3$ [22], and the compounded materials have shown good photocatalytic effects.

In this paper, $AgBiS_2$/BiOI composites were prepared by precipitation method based on the performance characteristics of BiOI and $AgBiS_2$. Simulated visible light degradation of RhB was used to evaluate the photocatalytic performance of the composites at different ratios, and the degradation results were also outstanding, with the materials achieving 94% degradation of 100 mg/L of pollutants within 180 min, and their photocatalytic performance was 1.4 and 4.5 times better than that of the BiOI and $AgBiS_2$ samples, respectively. This work provides a novel approach to the design and synthesis of composite materials for the efficient removal of organic pollutants.

2. Experimental

2.1. Materials

$Bi(NO_3)_3·5H_2O$(AR) was purchased from Tianjin Fuchen Reagent Company, KI(AR) was purchased from Shanghai Silver Iodine Chemical Company Limited, $AgNO_3$ was purchased from Shanghai Reagent No.1 Factory, THU was purchased from Tianjin Tianli Chemical Reagent Company, AO was purchased from Tianjin Hengxing Chemical Reagent, all the above reagents are AR.

2.2. Synthesis

Preparation of $AgBiS_2$/BiOI composites by co-precipitation method. The $AgBiS_2$ material was first prepared by the solvothermal method using EG as the solvent and $Bi(NO_3)_3·5H_2O$, $AgNO_3$ and THU as raw materials. 1 mmol $Bi(NO_3)_3·5H_2O$ and 1 mmol $AgNO_3$ were weighed into 15 ml of EG solution and stirred at room temperature until dissolved, then 3 mmol THU was added and stirring was continued for 2 h. Then 2 mmol AO was added and stirred until all materials were well mixed, and finally the materials were transferred to a 20 ml polytetrafluoroethylene reactor After the reaction, the sample was washed with deionised water and ethanol and dried under vacuum at 60°C for 6 h.

Then 1 mmol of $Bi(NO_3)_3·5H_2O$ was added to 20 ml of solvent mixture (ETH/EG=1/1) and sonicated for 30 min to dissolve the solution, then a certain mass ratio of $AgBiS_2$ was added to the solution and stirred for 10 min to mix the materials. Subsequently, 20 ml of aqueous KI solution (Bi^{3+}/I⁻=1/1) was added drop by drop to the above solution. The pH of the system was adjusted to neutral using 1.5 M $NH_3·5H_2O$ solution. After the reaction, the sample was washed with deionised water and ethanol and dried at 60 °C for 6 h. The reaction was carried out at 80 °C for 3 h.

2.3. Characterization

The crystalline phase structure of the prepared $AgBiS_2$/BiOI composites was characterised by using an X'Pert PRO type Cu-Kα diffractometer from Panalytical Analytical Instrument Company of the Netherlands. A field emission scanning electron microscope (FE-SEM, Sirion200,

Philip) and a transmission electron microscope (TEM, JEM2100, Japan) were used to observe and analyze the microstructure of the material. A 150W xenon lamp with a wavelength of 335 nm was used as an excitation source, and the photoluminescence spectrum (PL, RF-5301PC, Shimadzu, Japan) was measured at an excitation wavelength of 375 nm at room temperature.

2.4. Assessment of photocatalytic activity

Rhodamine B (100 mg/L) dye solution was selected as a degradant to evaluate the photocatalytic performance of $AgBiS_2$/BiOI composites. Prior to the photocatalytic experiments, 1 mg of catalyst was added to 100 mL of dye solution and placed under dark conditions with stirring for 1 h to achieve equilibrium in the adsorption of the material. A xenon lamp (300 W) was then switched on to simulate sunlight for the photocatalytic experiments. A UV-vis spectrometer (722N) was used to detect the change in RhB concentration over a 3 h period.

3. Results and discussion

Figure 1 presents the XRD diffraction patterns of samples BiOI, $AgBiS_2$ and different composite ratios of $AgBiS_2$/BiOI. The main diffraction peaks of BiOI at 2θ=29.6° and 31.7° match the standard card (JCPDS:10-0445), corresponding to the (102) and (110) faces of BiOI, respectively, with lattice parameters a=b=0.399 nm and c=0.915 nm. The main diffraction peaks of sample $AgBiS_2$ at 2θ=27.5° and 31.7° match the standard card (JCPDS:21-1178), corresponding to the (111) and (200) faces of the material, respectively, with lattice parameters a=b=c=0.565nm. For the XRD spectra of the composite $AgBiS_2$/BiOI material, the diffraction peaks of the sample BiOI and $AgBiS_2$ can be distinguished from each other, indicating that the structure of the material itself was not destroyed after the composite [23,24].

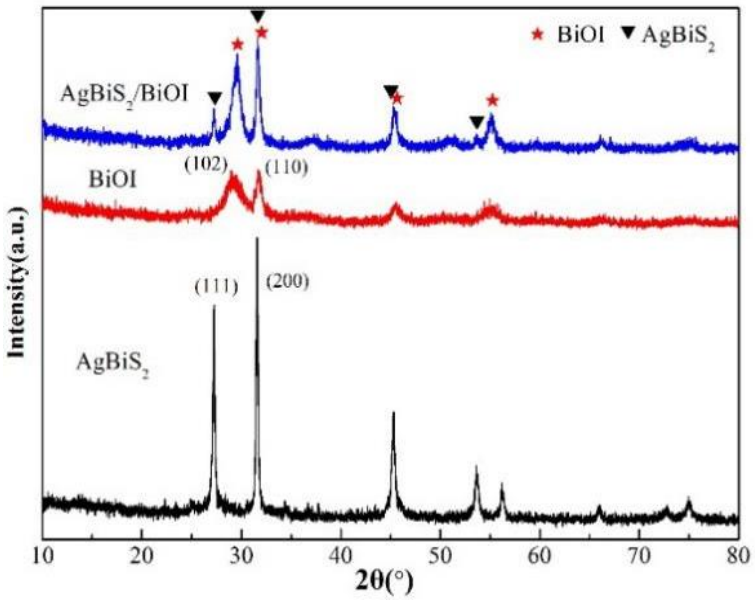

Fig. 1 XRD patterns of the BiOI, $AgBiS_2$ and $AgBiS_2$/BiOI composites.

Figure 2 presents scanning electron microscopy images (SEM) of the surface microstructures of samples BiOI and $AgBiS_2$/BiOI. It is clear from Fig. 2a that the BiOI material is a three-dimensional flower spherical structure, which has a great specific surface area and can enhance more photocatalytic active sites [25]. Fig.2b shows the SEM image of the $AgBiS_2$/BiOI composite, the structure of the material after its composite are irregular in shape, presumably the material is formed by the irregular assembly of BiOI and $AgBiS_2$. Fig. 2c shows an EDS image of the material, in which the elements contained in the composite are clearly shown.

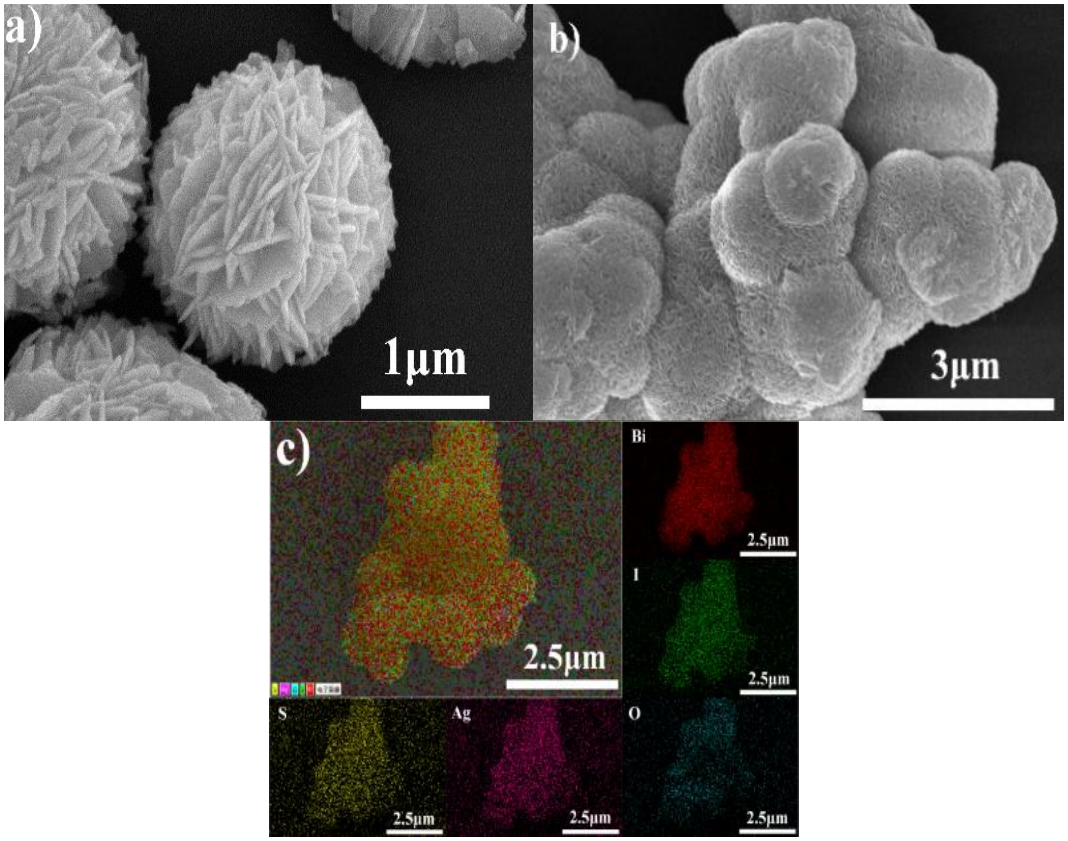

Fig. 2 SEM images of BiOI and $AgBiS_2$/BiOI composite materials and the elemental mapping images of Bi, O, I, Ag and S.

The morphological structure of the composite was further demonstrated by high resolution electron microscopy (HRTEM) as well as SAED images. As shown in Figure 3, the surface of the material can be seen in Figure a) to consist of a lamellar structure of BiOI with a lattice stripe d=0.30 nm corresponding to the (102) face of the material. The lattice stripe of the composite and the crystal plane spacing (d=0.28 nm) corresponding to the (110) and $AgBiS_2$ (200) faces of BiOI can be clearly distinguished from Fig. 3b, and the SAED diagram in Fig. 3c clearly shows the diffraction pattern of the material, which corresponds to the XRD diagram of the composite, proving that no impurities were produced after the material was compounded.

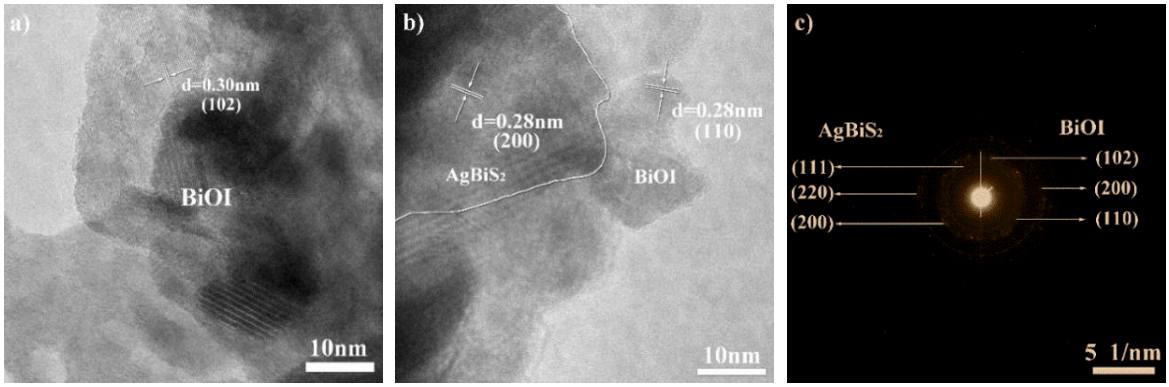

Fig. 3 HR-TEM and SAED diagrams of BiOI and $AgBiS_2$/BiOI composite materials.

The UV-Vis spectra of the different samples are shown in Figure 4. The energy band structure of the catalyst is calculated The energy band structure of the catalyst is calculated by the Tauc equation: $\alpha h\upsilon=A(h\upsilon-Eg)^{n/2}$, where α, h, A are the optical absorption coefficients, photon energies and scaling constants respectively, direct leap n=1 and indirect leap n=4. BiOI is usually an indirect leap, which in turn gives the band gap of BiOI as well as composites with different ratios. Where the band gap of the composites is reduced compared to the monomer, the results indicate the presence of $AgBiS_2$ material and that the energy band structure of the material after the composite is favourable for the response in visible light, for the photogenerated electron-hole separation and for improving the photocatalytic activity of the material.

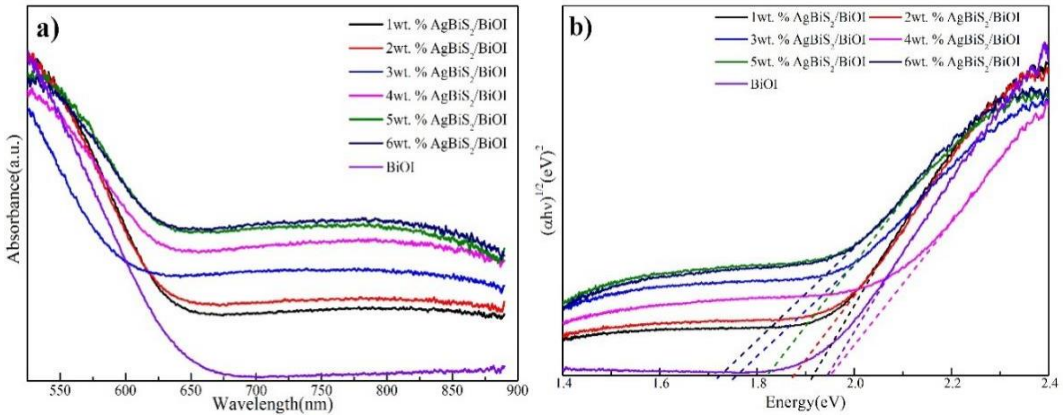

Fig. 4. UV-Vis reflectance spectrum a) and the relation curve between $(\alpha h\upsilon)^2$ and hυ b) of BiOI and $AgBiS_2$/BiOI composites.

The photocatalytic activity of the composites was evaluated by measuring the rate of degradation of the pollutant RhB by simulated visible light. This is shown in Figure 5a, where the degradation rate remains stable for the unadded catalyst, excluding the effect of RhB. It can be seen from the graph that the photocatalytic activity of the composites was significantly higher than that of the monomer. The 4wt. % $AgBiS_2$/BiOI material showed the best degradation rate of RhB within 3h of visible light irradiation, reaching 94%, significantly higher than that of pure BiOI (68%) and $AgBiS_2$ (21%), indicating that the $AgBiS_2$/BiOI composite has excellent photocatalytic activity.

The photocatalytic degradation rate of RhB by the composites followed the first order kinetic equation: $\ln(C_0/C_t)=kt$, where C_0 is the initial concentration of RhB, C_t is the concentration after a certain time of degradation, k is the rate constant and t is the reaction time. As shown in the graph, the composites showed significantly higher reaction rates than the monomer, with the rate constant k for the 4 wt. % $AgBiS_2$/BiOI material being approximately 0.0156 min^{-1}, which is 2.1 times higher than that for BiOI (0.0074 min^{-1}) and 10 times higher than that for $AgBiS_2$ (0.0016 min^{-1}). The results indicate that the composites can enhance the photocatalytic activity very well.

Figure 5c shows the fluorescence spectra of the pure BiOI and $AgBiS_2$/BiOI composites. The highest PL intensity of pure BiOI is seen in the figure, indicating the fast composite efficiency of the photogenerated carriers within the material, which is presumed to have poor photocatalytic activity. With the increasing addition of $AgBiS_2$, the fluorescence intensity gradually decreases, indicating that the formed composites can effectively inhibit the electron-hole complexation. The fluorescence intensity of the composites was lowest when the addition of $AgBiS_2$ was 4 wt. %, and it is presumed that the photocatalytic activity of the composites with this ratio is the best. The photocatalytic activity of the composites can be enhanced by effectively suppressing the compounding of photogenerated carriers as well as improving the transfer efficiency between interfacial charges. Figure 5d demonstrates the variation of EIS for BiOI, $AgBiS_2$ and $AgBiS_2$/BiOI. Where the radius of the arc of the composite $AgBiS_2$/BiOI is smaller than that of BiOI and $AgBiS_2$, this phenomenon indicates that the composite can facilitate the transfer of photosensitive charges across the interface of the semiconductor composite, which can enhance the

photocatalytic activity of the material [26]. From the above analysis, it is concluded that the results of PL and EIS remain consistent with the activity test results.

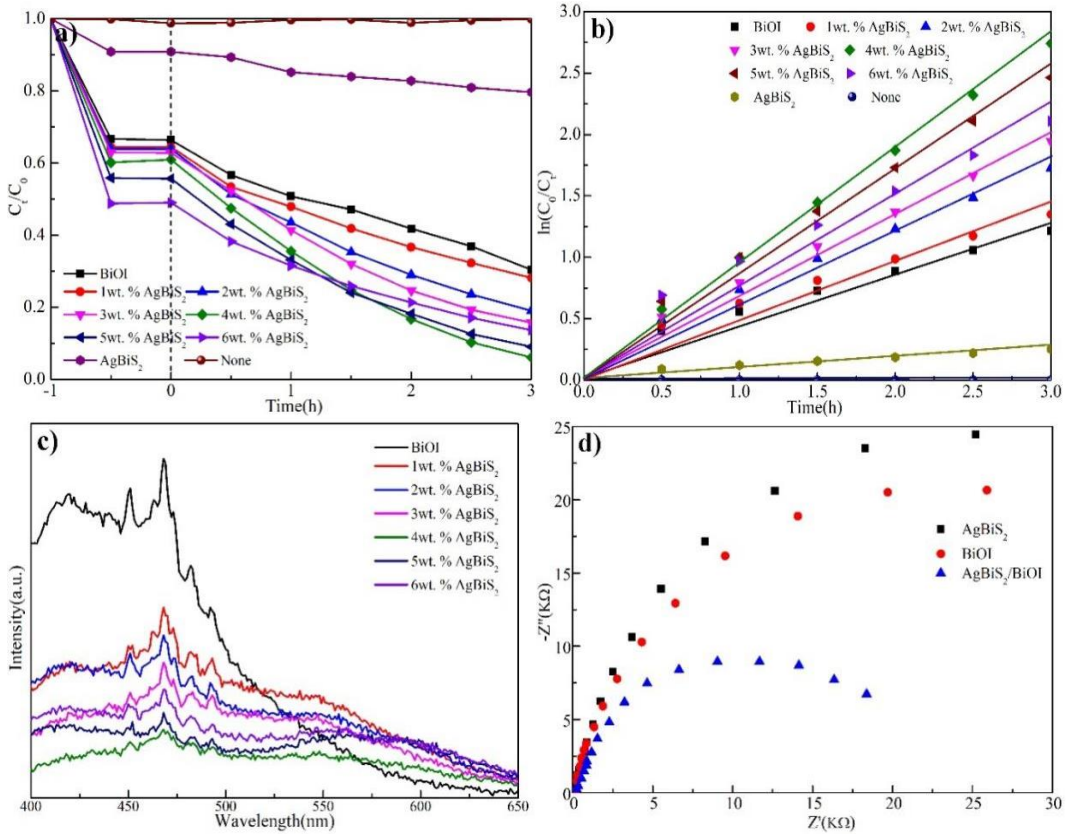

Fig. 5. BiOI, $AgBiS_2$ and $AgBiS_2$/BiOI samples tested for photocatalytic activity a), kinetic k-value b), PL c) and EIS d).

A recycling test on 4 wt. % $AgBiS_2$/BiOI was used to assess the stability of the composites. As shown in Figure 6a, the composites were still able to achieve a degradation rate of about 94% for RhB after 5 cycles, indicating that the prepared composites have good recyclability. Figure 6b shows the XRD spectrum after 5 cycles. The XRD pattern of the composites after cycling remains basically the same as that of the initial sample, which proves the good stability of the material. The above results indicate that the prepared composites have good stability and recyclability.

In order to analyse the photocatalytic mechanism of the prepared composites, the positions of the conduction band (CB) and valence band (VB) edges of the synthesised materials were calculated. Combined with UV-Vis DRS analysis, the band gaps (Eg) of BiOI and $AgBiS_2$ are 1.93 eV and 2.51 eV [21]. The positions of the conduction band and valence band of BiOI and $AgBiS_2$ can be calculated according to equations (3-7) and (3-8), which are shown below:

$$E_{CB} = \chi - E_C - 0.5E_g \tag{1}$$

$$E_{VB} = E_{CB} + E_g \tag{2}$$

where E_{CB} is the conductive potential and E_{VB} is the valence band potential. The χ values for BiOI and $AgBiS_2$ were calculated to be 4.76 and 5.33, respectively, and the E_{CB} was calculated to be -0.705 eV and -0.425 eV for BiOI and $AgBiS_2$, respectively, and the E_{VB} was 1.225 eV and 2.085 eV, respectively. Under simulated sunlight, the transfer of electrons and holes in the material is inferred as shown in Figure 7.

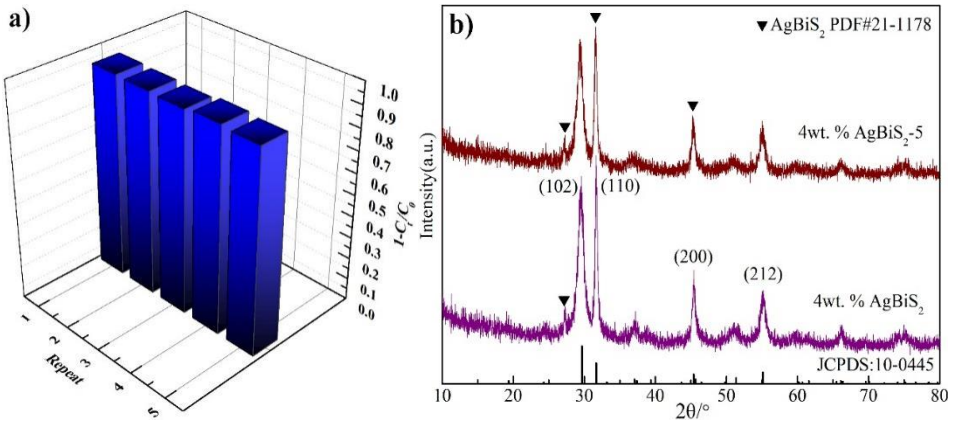

Fig. 6 Recycling test on the 4wt. % $AgBiS_2$/BiOI for the degradation of RhB.

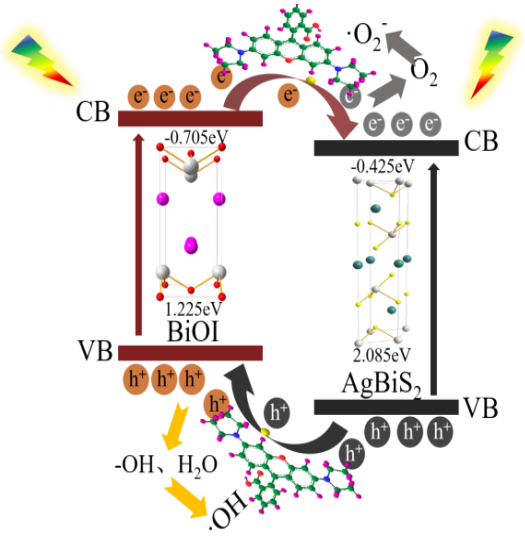

Fig. 7. Photocatalytic mechanism diagram of $AgBiS_2$/BiOI sample.

Inferred from the energy band position, $AgBiS_2$ and BiOI compound to form a traditional type II heterojunction. When the material is irradiated by sunlight, the BiOI material absorbs energy, and the electrons on VB will jump to CB, and the remaining electron vacancies will form h^+ with oxidation effect. The electrons transferred to the CB will be transferred to the CB of the $AgBiS_2$ material, causing the CB of the $AgBiS_2$ material to gather electrons, which has a strong reducing effect. The electrons on VB of $AgBiS_2$ material will jump to CB and generate holes, and the generated holes will be transferred to the VB position of BiOI material, so that the VB position of BiOI has a strong oxidation effect, which will react with hydroxyl to generate hydroxyl radicals. And the electrons that jump to the conduction band position of $AgBiS_2$ increase sharply, which strengthens the reduction effect of the material. The electrons at the CB position react with O_2 to produce O_2^- which further degrades the pollutant RhB. The catalytic pathway involved can be presumed to be the following reaction formula:

$$AgBiS_2/BiOI + h\nu \rightarrow AgBiS_2/BiOI(h^+ + e^-) \quad (3)$$

$$e^- + O_2 \rightarrow \cdot O_2^- \quad (4)$$

$$h^+ + H_2O \rightarrow \cdot OH + H^+ \quad (5)$$

$$\cdot O_2^- + 2H^+ \rightarrow 2 \cdot OH \quad (6)$$

$$h^+ + RhB \rightarrow intermedia\ tes \rightarrow CO_2 + H_2O \quad (7)$$

$$\cdot O_2^- + RhB \rightarrow intermedia\ tes \rightarrow CO_2 + H_2O \quad (8)$$

$$\cdot OH + RhB \rightarrow intermedia\ tes \rightarrow CO_2 + H_2O \quad (9)$$

4. Conclusions

The $AgBiS_2$ nanomaterials were prepared by the solvothermal method, followed by the preparation of $AgBiS_2$/BiOI composite photocatalytic materials in different ratios by the precipitation method. The composites showed good photocatalytic activity by photocatalytic activity test, with 4 wt. % $AgBiS_2$/BiOI showing the best photocatalytic activity of about 94%, which was significantly higher compared to pure BiOI (68%) and $AgBiS_2$ (20%). After 5 cycles of RhB degradation, it was found that the degradation rate of 4wt. % $AgBiS_2$/BiOI still reached 94% and the XRD pattern of the post-reaction samples remained consistent with the initial XRD pattern of the samples, indicating that the composites have good stability as well as reproducibility for the recycling of the materials for environmental protection.

Acknowledgements

This research was supported by “National Natural Science Foundation of China (NSFC, 52105332)”, “General Program of State Key Laboratory of Advanced Welding and Joining (AWJ-22M15)”, “The Open Foundation Guangxi Key Laboratory of Optical and Electronic Materials and Devices(20KF14)”, “Heilongjiang Province National Natural Science Foundation (E2018043)”, and “Project of Guangxi Base and Talents (AD19110086)”.

References

[1] J. H. Qu, M. H. Fan, Crit Rev Env Sci Tec. 40, 519 (2010); https://doi.org/10.1080/10643380802451953

[2] G. M. Zeng , M. Chen, Z. T. Zeng, Science. 340, 1403 (2013); https://doi.org/10.1126/science.340.6139.1403-a

[3] O. Ganzenko, D. Huguenot, E. D. van Hullebusch, G. Esposito, M. A. Oturan, Environ Sci Pollut R. 21, 8493 (2014); https://doi.org/10.1007/s11356-014-2770-6

[4] S. Ray, M. Takafuji, H. Ihara, RSC Advances. 3, 23664 (2013); https://doi.org/10.1039/c3ra43871f

[5] X. Zhou, Y. Li, Y. Zhao, RSC Advances. 4, 15620 (2014); https://doi.org/10.1039/C4RA00128A

[6] V. K. Gupta, I. Ali, T. A. Saleh, A. Nayak, S. Agarwal, RSC Advances. 2, 6380 (2012); https://doi.org/10.1039/c2ra20340e

[7] J. Sun, B. Zhang, R. Sun, Y. Li, J. Wu, International Journal of Environment and Pollution.

38, 81 (2010); https://doi.org/10.1504/IJEP.2009.026652
[8] H. Cheng, B. Huang, Y. Dai, Nanoscale. 6, 2009 (2014); https://doi.org/10.1039/c3nr05529a
[9] L. Ye, Y. Su, X. Jin, H. Xie, F. Cao and Z. Guo, Appl. Surf. Sci. 311, 858 (2014); https://doi.org/10.1016/j.apsusc.2014.05.191
[10] J. Di, J. Xia, H. Li, S. Guo, S. Dai, Nano Energy. 41, 172 (2017); https://doi.org/10.1016/j.nanoen.2017.09.008
[11] X. Zhang, B. Li, J. Wang, Y. Yuan, Q. Zhang, Z. Gao, L.-M. Liu, L. Chen, Physical Chemistry Chemical Physics. 16, 25854 (2014); https://doi.org/10.1039/C4CP03166K
[12] Y. Yang, C. Zhang, C. Lai, G. Zeng, D. Huang, M. Cheng, J. Wang, F. Chen, C. Zhou, W. Xiong, Advances in Colloid and Interface Science. 254, 76 (2018); https://doi.org/10.1016/j.cis.2018.03.004
[13] H. An, B. Lin, C. Xue, X. Q. Yan, Y. Z. Dai, J. J. Wei, G. D. Yang, Chinese Journal of Catalysis. 39, 654 (2018); https://doi.org/10.1016/S1872-2067(17)62927-9
[14] S. Y. Guo, H. H. Luo, Y. Li, J. Z. Chen, B. Mou, X. Q. Shi, G. X. Sun, Journal of Alloys and Compounds. 852, 157026 (2021); https://doi.org/10.1016/j.jallcom.2020.157026
[15] X. Y. Kong, W. Q. Lee, A. R. Mohamed, S.-P. Chai, Chemical Engineering Journal. 372, 1183 (2019); https://doi.org/10.1016/j.cej.2019.05.001
[16] M.E. Malefane, U. Feleni, P.J. Mafa, A.T. Kuvarega, Applied Surface Science. 514, 145940 (2020); https://doi.org/10.1016/j.apsusc.2020.145940
[17] F. Viñes, M. Bernechea, G. Konstantatos, F. Illas, Physical Review B. 94, 235203 (2016); https://doi.org/10.1103/PhysRevB.94.235203
[18] J. Zhong, W. Xiang, C. Xie, X. Liang, X. Xu, Materials Chemistry and Physics. 138, 773 (2013); https://doi.org/10.1016/j.matchemphys.2012.12.057
[19] T. Thongtem, N. Tipcompor, S. Thongtem, Materials Letters. 64, 755 (2010); https://doi.org/10.1016/j.matlet.2010.01.003
[20] P. Ganguly, S. Mathew, L. Clarizia, S. Kumar R, A. Akande, S. Hinder, A. Breen, S. C. Pillai, Applied Catalysis B: Environmental. 253, 401 (2019); https://doi.org/10.1016/j.apcatb.2019.04.033
[21] S. Paul, B. Dalal, R.Jana, et al. Journal of Physical Chemistry C. 124, 12824 (2020); https://doi.org/10.1021/acs.jpcc.0c03487
[22] Z. Liu, J, Liang, S. Li, S. Peng, Y. Qian, Chemistry-A European Journal. 10, 634 (2004); https://doi.org/10.1002/chem.200305481
[23] Z. Mao, J. Chen, Y. Yang, D. Wang, L. Bie, B. D. Fahlman, ACS Appl Mater Interfaces. 9, 12427 (2017); https://doi.org/10.1021/acsami.7b00370
[24] H. Cao, C. Jia, H. Zhang, G. Hou, Y. Tang, G. Zheng, New Journal of Chemistry. 45, 10608 (2021); https://doi.org/10.1039/D1NJ00707F
[25] D. Qian, S. Zhong, S. Wang, Y. Lai, N. Yang, W. Jiang, RSC Advances. 7, 36653 (2017); https://doi.org/10.1039/C7RA06116A
[26] L. W. Shan, J. C. Li, Z. Wu, L. M. Dong, H. T. Chen, D. Li, J. Suriyaprakash, X. L. Zhang, CHEM ENG J. 436, 131516 (2022); https://doi.10.1016/j.cej.2021.131516